REPORT DOCUMENTATION PAGE

Form Approved
OMB NO. 0704-0188

1. AGENCY USE ONLY (Leave Blank)	2. REPORT DATE	3. REPORT TYPE AND DATES COVERED
	24 January 2001	09/25/95 to 07/31/99 FINAL

4. TITLE AND SUBTITLE
SiGeC Optoelectronic Devices

5. FUNDING NUMBERS
DAAH04-95-1-0625

6. AUTHOR(S)
James Kolodzey

7. PERFORMING ORGANIZATION NAME(S) AND ADDRESS(ES)
Department of Electrical and Computer Engineering
University of Delaware
Newark, DE 19716

8. PERFORMING ORGANIZATION REPORT NUMBER

9. SPONSORING / MONITORING AGENCY NAME(S) AND ADDRESS(ES)

U. S. Army Research Office
P.O. Box 12211
Research Triangle Park, NC 27709-2211

10. SPONSORING / MONITORING AGENCY REPORT NUMBER
ARO 33074.1-EL

11. SUPPLEMENTARY NOTES
The views, opinions and/or findings contained in this report are those of the author(s) and should not be construed as an official Department of the Army position, policy or decision, unless so designated by other documentation.

12 a. DISTRIBUTION / AVAILABILITY STATEMENT
Approved for public release: distribution unlimited.

12 b. DISTRIBUTION CODE

13. ABSTRACT (Maximum 200 words)

The spectral responses of a series of heterojunction diodes of p-type $Ge_{1-y}C_y$ on n-type Si (100) substrates were measured by Fourier transform infrared spectroscopy. Alloy layers 0.5 μm thick were grown by molecular beam epitaxy at a substrate temperature of 400 °C and were doped p-type with different B concentrations. With increasing C content, the diode dark current decreased, and the optical absorption band edge shifted toward higher energy by 70 meV for 0.12 atomic % of C. The increase in energy was attributed to the composition dependence of the bandgap rather than to strain relaxation, because the GeC layers were nearly relaxed with the same strain. The photoresponsivity was 0.07 Amps/Watt at a wavelength of 1.55 μm, and 0.2 Amps/Watt at a wavelength of 1.3 μm. These measurements show that GeC photodetectors have good properties and reasonable response at technologically important near-infrared wavelengths and can be fabricated by heteroepitaxy for compatibility with Si integrated circuits.

14. SUBJECT TERMS	15. NUMBER OF PAGES
Silicon, germanium, carbon materials and devices, optoelectronic devices	13
	16. PRICE CODE

17. SECURITY CLASSIFICATION OR REPORT	18. SECURITY CLASSIFICATION ON THIS PAGE	19. SECURITY CLASSIFICATION OF ABSTRACT	20. LIMITATION OF ABSTRACT
UNCLASSIFIED	UNCLASSIFIED	UNCLASSIFIED	UL

MASTER COPY: PLEASE KEEP THIS "MEMORANDUM OF TRANSMITTAL" BLANK FOR REPRODUCTION PURPOSES. WHEN REPORTS ARE GENERATED UNDER THE ARO SPONSORSHIP, FORWARD A COMPLETED COPY OF THIS FORM WITH EACH REPORT SHIPMENT TO THE ARO. THIS WILL ASSURE PROPER IDENTIFICATION. NOT TO BE USED FOR INTERIM PROGRESS REPORTS; SEE PAGE 2 FOR INTERIM PROGRESS REPORT INSTRUCTIONS.

MEMORANDUM OF TRANSMITTAL

U.S. Army Research Office
ATTN: AMSRL-RO-BI (TR)
P.O. Box 12211
Research Triangle Park, NC 27709-2211

☐ Reprint (Orig + 2 copies)
☐ Technical Report (Orig + 2 copies)
☐ Manuscript (1 copy)
☒ Final Progress Report (Orig + 2 copies)
☐ Related Materials, Abstracts, Theses (1 copy)

CONTRACT/GRANT NUMBER: DAAH04-95-1-0625

REPORT TITLE: SiGeC optoelectronic Devices

is forwarded for your information.

SUBMITTED FOR PUBLICATION TO (applicable only if report is manuscript):

Sincerely,

REPORT DOCUMENTATION PAGE (SF298)
(Continuation Sheet)

Infrared photodetectors for the optical fiber communication wavelengths of 1.3 and 1.55 microns are typically made of Ge or InGaAs. Epitaxial infrared detectors on Si substrates are attractive for circuit integration, provided that the detector properties and the reliability are adequate. The 4% lattice mismatch of epitaxial Ge on Si produces strain that relaxes by dislocation and defect formation in thick layers. The addition of C to Ge reduces the strain thus limiting the formation of dislocations, and also reduces the diffusion of dopants. The effects of C on device properties are not yet well understood. The optical and electrical characteristics of GeC photodiodes are therefore interesting both fundamentally and technologically. We report here on measurements of the photoresponse of GeC/Si heterojunction photodiodes on Si substrates, to determine if the layers are suitable for device applications.

Device Fabrication

The p-doped GeC layers were grown by solid source molecular beam epitaxy (MBE) at 400 °C using methods described elsewhere. The substrates were n-type Si (100) with a doping concentration of 3×10^{15} cm^{-3}. The Ge source was a thermal effusion cell operating from 1310 °C to 1325 °C with a pyrolytic boron nitride (pBN) crucible. The C source was a pyrolytic graphite filament heated by currents up to 48 Amps. The p-type dopant source was a high temperature effusion cell containing elemental B in a crucible of pyrolytic graphite in a W metal jacket, operating from 1450 °C to 1650 °C. The alloy growth rate was 1.5 nm/min. No surfactants such as atomic H were used during growth, and no changes in growth rate with doping or composition were observed. The layers were 560 nm thick, except for one sample that was 520 nm thick (SGC-84 in Table I).

Table I. Properties of the $Ge_{1-y}C_y$ layers used in the p-N heterojunction photodiodes, including composition, B doping level, forward current ideality factor, bandgap energy, phonon energy and strain. The n-type Si (001) substrates had a doping level of 3×10^{15} cm^{-3}. The hole carrier concentrations are listed beneath the B impurity concentrations. The layer thickness was 560 nm for all samples except SGC-84, which was 520 nm thick. The Ge diode is a commercial bulk Ge homojunction as described in the text.

Sample	C content (atomic %)	B conc. hole conc. (cm^{-3})	Forward ideality factor	E_g (eV)	E_{ph} (meV)	Strain
Ge diode	0		-	0.639	10	-
SGC102	0	B: 1.2×10^{17} p: 7.5×10^{17}	1.04	0.657	14	2.8×10^{-3}
SGC103	0	B: 1.2×10^{19} p: 1.8×10^{19}	1.84	0.634	17	2.4×10^{-3}
SGC80	0.06%	B: 3×10^{18} p: 2.5×10^{18}	1.22	0.731	11	2.7×10^{-3}
SGC81	0.08%	B: 4×10^{17} p: 6.8×10^{17}	1.09	0.741	11	3.1×10^{-3}
SGC82	0.11%	B: 3×10^{19} p: 1.1×10^{19}	1.08	0.715	12	3.2×10^{-3}
SGC84	0.12%	B: 5×10^{18} p: 1.9×10^{18}	1.01	0.728	11	2.6×10^{-3}

X-ray diffraction indicated that the epitaxial layers were single-crystals oriented to the substrate. Measurements of the symmetric and asymmetric x-ray reflections indicated that the strain was near 10^{-3} so that the alloy layers were nearly relaxed. In Table I, the strain is given by the difference between the perpendicular and parallel lattice constants divided by the relaxed lattice constant. The substitutional C fractions given in Table I were obtained from the effective lattice constants of fully relaxed alloys deduced by analyzing the x-ray diffraction measurements. A linear relation was assumed for the dependence of the alloy lattice constant on composition for the $Ge_{1-y}C_y$. It is possible that the total C fraction may be higher than the substitutional values quoted here due to bowing in the relation between lattice constant and composition. RBS ion channeling performed on

similar samples with higher C contents indicated that at least 80% of the C occupied substitutional lattice sites. The material quality of the layers was reported previously, and indicated that the layer/substrate interface had defects including twins.

The B doping concentration was measured using secondary ion mass spectrometry (SIMS). SIMS profiling showed that the doping was constant versus depth. Measurements across the wafer surface indicated that the doping level was uniform within 10% over a lateral distance of 1 cm. Table I gives the physical properties of the samples. For the same growth conditions, there is a slight trend of higher B concentration with C fraction, possibly due to an increase in the sticking coefficient of B with C, or perhaps to an artifact due to composition-dependent yields with SIMS. Hall effect measurements yielded the hole carrier concentrations (p) given in Table I that were reasonably close to the B doping concentration except for sample SGC-102, perhaps due to experimental error.

Mesa diodes with a junction area of 0.2 mm^2 and a light sensitive area (not shaded by the contacts) of 0.182 mm^2 were fabricated using photolithography and wet chemical etching. Electrical contacts of Ti/Au metal were thermally evaporated to a thickness of 60 nm/300 nm respectively, as shown in the inset to Fig. 1.

Electrical Measurements

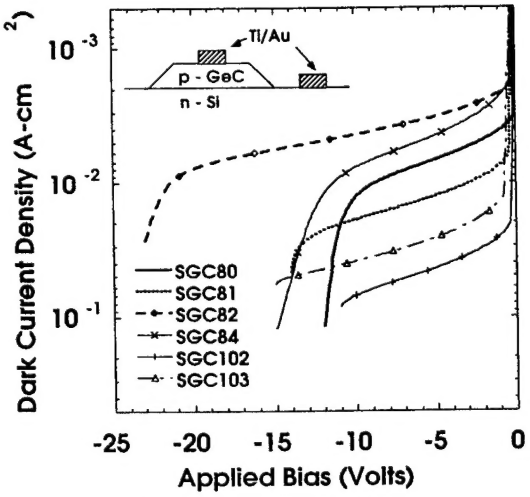

Figure 1. Dark current density versus reverse bias voltage of p-N type $Ge_{1-y}C_y$ /Si heterojunction diodes on Si (001) substrates with different composition and doping, given in Table I. The reverse leakage currents decreased significantly with C fraction and with doping concentration. The inset shows the diode structure.

Current-voltage measurements at room temperature showed rectifying characteristics, with reverse breakdown voltages ranging from 11 to 24 V, as in Fig 1. The reverse leakage dark current decreased significantly with increasing C content and with increasing hole concentration. In photodiode applications, a low dark current produces less noise and improves the detectivity. The decrease in dark current with C content was attributed to reductions in the bulk and surface recombination rates, possibly due to: (1) a decrease in the intrinsic carrier concentration n_i in the GeC layer, (2) a reduced dislocation density due to strain compensation, and (3) changes in the energy bandgap and band offsets. The diode p-n junctions were exposed on the mesa sidewalls, and an extra processing step of passivating the junctions with SiO_2, for example, may help reduce the dark current.

For completeness, the forward bias ideality factors are included in Table I, although it is not our intent to report here on the forward bias characteristics of the diodes. Ideality factors near 1 imply diffusion current, and ideality factors near 2 imply recombination current. Due to the high series resistance of the diodes, the values given here were obtained at small forward bias and may have significant error. A more highly doped substrate and different contact metals may help reduce the series resistance.

Optical Measurements

The spectral response of the photodiodes was measured at room temperature using a Biorad FTS-60A Fourier transform infrared spectrometer (FTIR) over the spectral range from 6000 to 10,000 cm^{-1}, using a quartz beam splitter and a glowbar light source. FTIR resolutions of 16 to 32 cm^{-1} were used for these measurements. The FTIR spectrometer was equipped with a UMA 500 microscope, and the photodiodes were inserted into the microscope beam path, using needle probes for electrical contact. To reduce the contribution of the Si substrate to the diode photocurrent, a high resistivity Si wafer, polished on both sides, was placed in the FTIR beam path to remove photon energies above 1.1 eV. A low impedance current-to-voltage amplifier (Hewlett-Packard 4140B) that was ac-coupled to the FTIR electronics collected the diode photocurrent. The ac-coupling of the measured signal yields the photocurrent, with the dc dark current removed. The diode photocurrent was referenced to the measured reflectivity of a thick Au metal pad located on each photodiode sample. The Au reflectivity was measured using the mercury cadmium telluride (MCT) detector of the FTIR microscope, which was calibrated by a pyroelectric (DTGS) detector having flat response versus wavelength. This procedure corrected the possible variations in instrument alignment and drift. The error was below 3 meV, based on consecutive measurements of the same diode. A commercial bulk Ge photodetector with known calibration was measured as a reference for the absolute responsivity. The commercial photodiode was a homojunction of Ge with an area of 8×10^{-3} cm^2, and a dark current of 2.5×10^{-3} $A\text{-}cm^{-2}$ at a bias of -3 V.

Fig. 2 shows the photoresponsivity versus photon energy for diodes with different alloy compositions and with hole concentrations ranging from 10^{17} to 10^{18} cm^{-3} (see Table I). The diodes were biased at -3 V. As seen, the responsivity values are respectable, considering that the GeC active layers are relatively thin. The strong responsivity above 0.8 eV was attributed to absorption by the direct energy valley of the alloy. In comparison, the responsivity of a thick bulk Ge photodiode followed the same energy dependence as that of the Ge/Si diodes near the indirect bandgap of Ge (E_g = 0.66 eV), reaching a maximum of 0.7 Amps/Watt at 0.8 eV and then slightly decreasing due to surface absorption. At energies near the fundamental bandgap of Ge, the onset of photoresponse regularly increased in energy with C concentration. A comparison of diodes having the same doping level yielded an increase in the absorption energy of ≈ 70 meV due to the presence of 0.12 atomic % C. Since the GeC alloy layers were thick and nearly relaxed with similar residual strain, the shift in absorption energy was attributed to the alloying effect of C, rather than to strain compensation. The Si layer is relatively transparent at these wavelengths, and the photoresponse was attributed fully to the GeC layer. At zero bias, the diodes showed a similar increase in absorption energy with C, but the responsivity magnitude was about half that at -3 V bias at all wavelengths. The lower photoresponse was attributed to the narrower depletion width at zero bias, and to less efficient charge collection at the lower electric field. In these junction photodiodes, the photogenerated charge is collected both within the depletion region and within a diffusion length of the depletion edge.

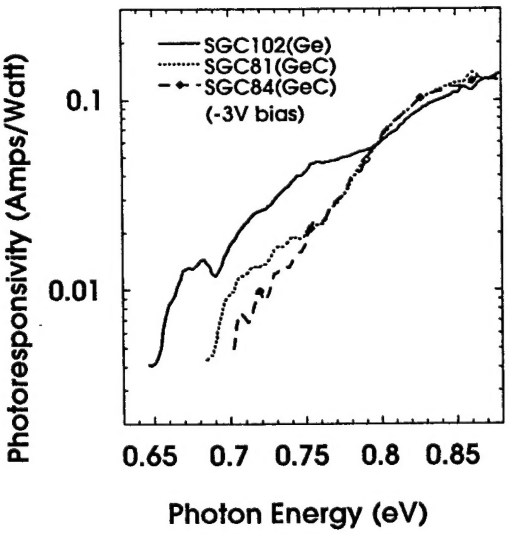

Figure 2. Spectral responsivity of $Ge_{1-y}C_y$ /Si p-N heterojunction diodes with different C fractions at -3V reverse bias. All $Ge_{1-y}C_y$ layers had nearly the same strain and thickness (as in Table I). The samples shown here had hole concentrations from 10^{17} to 10^{18} cm^{-3}. The blue-shifted absorption was attributed to the alloying effect of C as indicated by the bandgaps in Table I. For a given C content, the bandgap energies

decreased with doping concentration, as explained in the text. At zero bias, the spectral responsivity of all the diodes was reduced to about half of the magnitude at -3V.

The photoresponsivities of two samples with hole concentrations near 10^{19} cm^{-3} (SGC-103 and SGC-82) were shifted to slightly lower energies relative to the more lightly doped samples. The explanation may be found in bandgap renormalization, which decreases the absorption edge in semiconductors, and to impurity band absorption. The highly doped samples have a lower responsivity at all energies, attributed to their smaller depletion widths and diffusion lengths.

The results of Fig. 2 were exploited to estimate the indirect bandgap energy of the GeC absorbing layer of the photodiodes. For diodes with an optical absorbing width W that is less than the absorption depth $1/\alpha$ (the reciprocal of the optical absorption coefficient), the photocurrent density is approximately $J_{ph} = q\,(1\text{-}R)\,P\,\alpha W/h\nu$, where q is the magnitude of the electron charge, R the surface optical reflectivity, P the incident optical power density, and $h\nu$ the photon energy. For energy bands that are indirect in **k** space, the absorption coefficient follows the Macfarlane-Roberts expression for single phonon emission and absorption, with energy dependence given by:

$$\alpha = A\left[\frac{\left(h\upsilon - E_g - E_{ph}\right)^2}{1 - e^{-E_{ph}/kT}} + \frac{\left(h\upsilon - E_g + E_{ph}\right)^2}{e^{E_{ph}/kT} - 1}\right]$$

which holds for photon energies such that

$$h\upsilon > E_g + E_{ph}$$

with phonon energy E_{ph}, thermal energy kT, and where A is a constant.

In principle, a plot of the square root of photocurrent versus $h\nu$ can yield two linear slopes that extrapolate to zero absorption giving $E_g \pm E_{ph}$. Due to the weak photocurrent at energies near the bandgap, however, this procedure can give significant error. As a more comprehensive approach, we curve-fit the full Macfarlane-Roberts expression with the bandgap energy and the phonon energy as fitting parameters. The results of the fits for E_g and E_{ph} are reported in Table I. The values obtained for E_{ph} are consistent with the results of high-

resolution optical absorption studies in Ge indicating that acoustic phonons are more strongly involved than optical phonons.

The increase in the absorption edge with the addition of C is consistent with previous studies of Ge-rich alloys. An increase of 63 meV per at. % C was previously obtained from optical transmission measurements of unstrained GeC alloys. An increase of 43 meV per at. % C for the E_1 critical point near the L minimum was obtained by spectroscopic ellipsometry after correcting for strain. Assuming a deformation potential of 10 eV, the variation in strain between the samples would account for at most 8 meV of the observed bandgap differences. The reduction in the diode dark current by about a factor of 10 is consistent with the observed 70 meV increase in bandgap, because the leakage caused by recombination is proportional to the square of the intrinsic carrier concentration, n_i^2, which decreases exponentially with bandgap energy. It is also possible, however, that the lower leakage is due to a reduction in the dislocation density by C-induced strain compensation. Fig. 3 summarizes the dependence of the bandgap on composition and doping obtained from the curve fittings of the photoresponses. The reason for the initial strong increase in bandgap for small C fractions is not clear, but may indicate a strong bowing in the relation of bandgap to composition, or to the effects of carrier transport on the photoresponse.

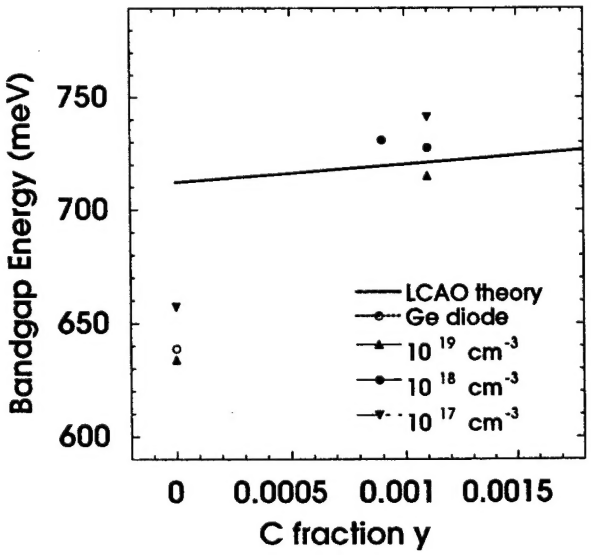

Figure 3. The dependence of bandgap energy (E_g) on C faction and doping level. The solid symbols give the doping concentrations measured by SIMS. The data points give E_g for the samples of Table I, obtained by fitting the measured diode photocurrents to the Macfarlane-Roberts expression for phonon-assisted absorption. The variations in E_g at particular C fractions are not due to experimental uncertainty, but show the decrease of

E_g with doping. For comparison purposes only, the solid line gives the theoretical E_g calculated by the LCAO method using the virtual crystal approximation, with a slope of 25.7 meV per at. % C. For brevity, the doping concentrations listed in the legend are approximate; the precise values are given in Table I.

Included in Fig. 3 is the result of theoretical calculations of E_g reported previously based on the virtual crystal approximation (VCA) using the linear combination of atomic orbitals (LCAO) method. This theory predicts an increasing bandgap with C fraction, although the VCA approach has the limitations of not accounting for strain localized about the C atom, nor to energy band broadening from alloy disorder. The theoretical curve was included for comparison; not as a claim for the validity of the VCA approximation. For Ge-rich alloys, the increase in bandgap with C is opposite to the decreases in bandgap for Si-rich alloys reported from measurements, and from predictions based on first principles calculations. These opposing effects of C with composition may involve the differences in the behavior of the L minimum for Ge versus the X minimum for Si.

The Macfarlane-Roberts expression for α accurately fit the diode photoresponses for energies above the indirect bandgap of Ge. The bandgap of diode SGC102 diode was in good agreement with the commonly accepted value for Ge. The bandgap measured for the commercial Ge diode was in-between that obtained for the Ge/Si diodes SGC102 and SGC103. Although the doping of the commercial Ge diode was not known, a possible reason for its bandgap could be that it has a doping level in-between that of the two SGC Ge diodes.

In summary, the electrical and optical measurements showed that $Ge_{1-y}C_y$ /Si heterojunction photodiodes have a responsivity that is attractive for practical applications. The photodiodes were fabricated by heteroepitaxy using MBE at low temperatures for compatibility with Si integrated circuit technology. Alloying with C increased the bandgap energy of $Ge_{1-y}C_y$, which was attributed to composition effects rather than to strain compensation because the layers were nearly relaxed. The variable bandgap can be useful for tuning the desired operating wavelengths of photodetectors and for reducing unwanted signals without sacrificing detector performance at important optical fiber communication wavelengths such as 1.55 and 1.3 μm. The reduction in dark current by adding C to Ge can improve the signal to noise ratio of optical receivers.

References:

1. H. Feng, M. Dashiell, B. A. Orner, J. Kolodzey, P. R. Berger, M.H. Ervin, and R.T. Lareau, ``Boron Diffusion in SiGeC Alloys Grown on a Silicon Substrate," 39th Electronic Materials Conference, Fort Collins, CO, June 25-27 (1997)

2. J. Kolodzey, P.A. O'Neil, S. Zhang, B. A. Orner, K. Roe, K.M. Unruh, C.P. Swann, M.M. Waite and S. Ismat Shah, ``Growth of germanium-carbon alloys on silicon substrates by molecular beam epitaxy,'' *Appl. Phys. Lett.*, vol. 67, pp. 1865-1867, 1995.

3. B. A. Orner, A. Khan, D. Hits, F. Chen, K. Roe, J. Pickett, X. Shao, R.G. Wilson, P. R. Berger and J. Kolodzey, ``Optical properties of GeC alloys,'' J. Electronic Materials, vol. 25, pp. 297-300, 1996.

4. B. A. Orner, J. Olowolafe, K. Roe, J. Kolodzey, T. Laursen, J. W. Mayer and J. Spear, ``Bandgap of Ge-rich SiGeC alloys,'' *Appl. Phys. Lett.*, vol. 69, pp. 2557-2559, 1996.

5. F. Chen, R. T. Troeger, K. Roe, M. D. Dashiell, R. Jonczyk, D.S. Holmes, R.G. Wilson and J. Kolodzey, ``Electrical properties of SiGeC and GeC alloys," *J. Electronic Materials.*, v. 26, pp. 1371-1375, 1997.

6. F. Chen, B. A. Orner, D. Guerin, A. Khan, P. R. Berger, S. Ismat Shah, and J. Kolodzey, ``Current transport characteristics of SiGeC/Si heterojunction diodes,'' IEEE Electron Device Lett., v. 17, pp. 589-591, 1996.

7. B. A. Orner, and J. Kolodzey, ``SiGeC alloy band structures by linear combination of atomic orbitals,'' J. Appl. Phys., v. 81, pp. 6773-6780, 1997.

8. J. Kolodzey, O. Gauthier-Lafaye, S. Sauvage, J.-L. Perrossier, P. Boucaud, F.H. Julien, J.-M. Lourtioz, F. Chen, B. A. Orner, K. Roe, C. Guedj, R.G. Wilson, and J. Spear, "The effects of composition and doping on the response of GeC/Si photodiodes, " *IEEE J. Selected Topics in Quantum Electronics*, v. 4, pp. 964-969, Nov./Dec. 1998.

9. Xiaoping Shao, Ralf Jonczyk, M. W. Dashiell, D. Hits, B. A. Orner, A-S. Khan, K. Roe, J. Kolodzey, Paul R. Berger, M. Kaba, M. A. Barteau, and K. M. Unruh, "Strain modification in thin $Si_{1-x-y}Ge_xC_y$ Alloys on (100) Si for formation of high density and uniformly sized quantum dots," *J. Appl. Phys.*, v. **85**, pp. 578-582, 1999.

10. R. Duschl, O. G. Schmidt, W. Winter, K. Eberl, M. W. Dashiell, J. Kolodzey, N. Y. Jin-Phillipp and F. Phillipp, ``Growth and thermal stability of pseudomorphic $Ge_{1-y}C_y$ /Ge superlattices on Ge (001)," *Appl. Phys. Lett.*, v. 74, pp. 1150-1154, 1999.

11. L. V. Kulik, C. Guedj, M. W. Dashiell, J. Kolodzey, and A. Hairie, ``The phonon spectra of substitutional carbon in SiGe alloys," *Physical Review B*, v. 59, pp. 15753-15759, 1999.

12. K. Roe, M. W. Dashiell, J. Kolodzey, C. Guedj, P. Boucaud and J.-M. Lourtioz, `` The MBE growth of $Ge_{1-y}C_y$ alloys on Si (100) with high carbon contents, " *J. Vac. Sci. Technol.* B, vol. 17, pp. 1301-1303, May/June, 1999.